



## Efficient synthesis and antioxidant activity of novel *N*-propargyl tetrahydroquinoline derivatives through the cationic Povarov reaction



Yeray A. Rodríguez Núñez<sup>a</sup>, Maximiliano Norambuena<sup>a</sup>, Arnold R. Romero Bohórquez<sup>b</sup>, Alejandro Morales-Bayuelo<sup>c</sup>, Margarita Gutiérrez<sup>a,\*</sup>

<sup>a</sup> Laboratorio Síntesis Orgánica, Instituto de Química de Recursos Naturales, Universidad de Talca, Casilla 747, Talca, 3460000, Chile

<sup>b</sup> Grupo de Investigación de Compuestos Orgánicos de Interés Medicinal (CODEIM), Parque Tecnológico Guatiguará, Universidad Industrial de Santander, A.A. 678, Piedecuesta, Colombia

<sup>c</sup> Centro de Investigación de Procesos del Tecnológico Comfenalco (CIPTEC), programa de Ingeniería Industrial, Fundación Universitaria Tecnológico Comfenalco – Cartagena, Cr 44 D N 30A, 91, Cartagena-Bolívar, Colombia

### ARTICLE INFO

#### Keywords:

Organic chemistry  
Theoretical chemistry  
Pharmaceutical chemistry  
Tetrahydroquinolines  
Propargylamines  
Antioxidant activity  
Free radical  
Molecular quantum similarity measure

### ABSTRACT

New *N*-propargyl tetrahydroquinolines **6a-g** have been synthesized efficiently through the cationic Povarov reaction (a domino Mannich/Friedel-Crafts reaction), catalyzed by Indium (III) chloride (InCl<sub>3</sub>), from the corresponding *N*-propargylanilines preformed, formaldehyde and *N*-vinylformamide, with good to moderate yields. All tetrahydroquinoline derivatives obtained were evaluated *in vitro* as free radical scavengers. Results showed that compound **6c** presents a potent antioxidant effect compared with ascorbic acid, used as a reference compound. ADME predictions also revealed favorable pharmacokinetic parameters for the synthesized compounds, which warrant their suitability as potential antioxidants. Additionally, a theoretical study using Molecular Quantum Similarity and reactivity indices were developed to discriminate different reactive sites in the new molecules in which the oxidative process occurs.

### 1. Introduction

In the research of biologically active molecules, free radicals have been linked to several degenerative diseases including neurodegenerative and cardiovascular disorder, atherosclerosis and cancer (Aruoma, 1998). Although the discovery of antioxidant compounds has been an area widely studied (Kouznetsov et al., 2011; Bulut et al., 2018; Martelli and Giacomini, 2018) it is necessary to continue in the search of new natural or synthetic compounds that can act as free radical scavengers and help in the treatment or control of diseases related to oxidative stress.

Heterocyclic compounds, especially nitrogen heterocycles, are a very important class of compounds with application in the pharmaceutical industries, which comprise about 60% of all pharmacological substances. The tetrahydroquinoline (THQ) ring system, in particular, is a common structural motif found in numerous biologically active natural products showing broad biological activities (Nammalwar and Bunce, 2014). Because of the significance of these scaffolds in drug discovery and medicinal chemistry, the development of new methodologies for the synthesis of THQs derivatives continues to be an active field of investigation, as is evidenced by the appearance of over 400 research articles in this

area during the last years (Sridharan et al., 2011; Katritzky et al., 1996).

In the last decades, a great number of synthetic methods for access to THQs derivatives have been reported (Sridharan et al., 2011). In many cases, these methodologies involve an intramolecular Friedel-Crafts reaction of *N*-substituted anilines with a suitable functional group bound to the nitrogen atom (Abonia et al., 2013). In this sense, the use of multi-component Povarov reaction, catalyzed by Lewis or Brønsted acids between *N*-arylimines (obtained from anilines and aryl (alkyl)aldehydes) and electron-rich alkenes, is maybe the most powerful tool that provides quick and efficiently THQ scaffold with great structural diversity. Recently, we have been successfully exploring the cationic version of the Povarov reaction (a domino Mannich/Friedel-Crafts reaction). This method resulted highly efficient to access different *N*-derivatives of THQs (Romero Bohórquez et al., 2016; Acelas et al., 2017), including the synthesis of new *N*-allyl/propargyl 1,2,3,4-THQs, promissory dual inhibitors against AChE and BChE enzymes (Rodríguez et al., 2016).

Diverse amine derivatives with the propargyl fragment in its structure are versatile compounds with demonstrated pharmacological and pharmaceutical applications such as antioxidant agents (Dragoni et al., 2006) and as inhibitors of some monoamine oxidases MAO-B. Selegiline,

\* Corresponding author.

E-mail address: [mgutierrez@utalca.cl](mailto:mgutierrez@utalca.cl) (M. Gutiérrez).

<https://doi.org/10.1016/j.heliyon.2019.e02174>

Received 22 May 2019; Received in revised form 17 July 2019; Accepted 25 July 2019

2405-8440/© 2019 Published by Elsevier Ltd. This is an open access article under the CC BY-NC-ND license (<http://creativecommons.org/licenses/by-nc-nd/4.0/>).

Rasagiline, Pargyline, and Ladostigil drugs are widely used as enzymatic inhibitors in treatments of neurodegenerative diseases (Fig. 1) (Baranyi et al., 2016; Bolea et al., 2013; Mao et al., 2015). Taking into account all the above, in the present study, we report the synthesis, spectroscopic characterization and antioxidant activity of a new series of *N*-propargyl-THQs obtained via mild and expeditious  $\text{InCl}_3$  catalyzed-cationic Povarov reaction. Results indicated that some THQs derivatives evaluated showed good activity as potential free radical scavengers. In addition, theoretical studies of Molecular Quantum Similarity Measure allowed explaining the biological activity reported. Local reactivity descriptors like the local softness and electrophilicity indices were obtained with the help of Fukui function calculation.

## 2. Results and discussion

The preparation of new *N*-propargyl THQs **6a-g** via domino Mannich addition/Friedel-Crafts intramolecular alkylation reactions catalyzed by  $\text{InCl}_3$ , was effective under mild condition reactions using *N*-propargylamines with formaline (37% in methanol) and *N*-vinylformamide as an electron-rich alkene. Acetonitrile ( $\text{CH}_3\text{CN}$ ) was used as solvent based on previous reports (Romero Bohórquez et al., 2016; Abonia et al., 2013). Synthetic route and structures of final compounds are shown in Scheme 1. According to the results, although fluctuations in the reaction yield were shown, in general, the reaction showed to be powerful synthetic strategy to obtain the corresponding 1,2,3,4-THQ compounds with high structural diversification (Table 1).

All new *N*-propargyl THQ derivatives **6a-g** were obtained as stable solids and were characterized by IR,  $^1\text{H-NMR}$ ,  $^{13}\text{C-NMR}$ , and MS. In the IR spectra, C=O vibration bands ( $1643\text{--}1658\text{ cm}^{-1}$ ) and propargyl fragment vibration bands ( $3231\text{--}3279\text{ cm}^{-1}$ ) were observed.  $^1\text{H NMR}$  spectral analysis of the synthesized *N*-propargyl tetrahydroquinolines showed four groups of characterized signals. First, signals between 6.88–7.31 ppm indicated the presence of aromatic protons corresponding to the tetrahydroquinoline ring. Also was possible to observe the aliphatic proton signals, around 5.10–1.99 ppm, corresponding to THQ nucleus and the signal for the alkyne proton between 2.13–2.28 ppm. Finally, around 8.11–8.21 ppm, proton signal for formamide group was observed. This set of signals constitutes evidence that the formation of the tetrahydroquinoline compounds took place favorably.  $^1\text{H}$  and  $^{13}\text{C}$  nuclear magnetic resonance (NMR) spectra of compound **6a-6g** are included in supplementary material (Fig S1-FigS7).

The presence of a fragment *N*-propargyl in the new compounds is interesting owing to propargylamines are useful synthetic precursors in the obtaining of different organic substrates, natural products, and drugs as evidenced by the large number of articles published in the literature

(Hua and Nizami, 2018; Lauder et al., 2017; Yang et al., 2018). The versatility of propargylamines is due to its unique structure composed of an amine group in  $\beta$ -position to an alkyne moiety. Compounds with a carbon–carbon triple bond have characteristic reactivity and can behave as electrophilic substrates and as an electron source in nucleophilic reactions (Mao et al., 2015). It is worth noting that, as mentioned above, some *N*-propargyl derivatives have been applied mainly as monoamine oxidase inhibitors (MAO) and, according to the literature, could promote antioxidant effects by acting as radical scavengers (Dragoni et al., 2006).

All compounds obtained were evaluated as antioxidant agents in presence of the stable radical DPPH (1,1-diphenyl-2-picrylhydrazyl) at a concentration ranging from 10 to 100  $\mu\text{L}$  and compared with ascorbic acid as shown in Table 2. The DPPH scavenging activity varied greatly. There were no clear differences in  $\text{IC}_{50}$  values between the compounds synthesized despite the presence of substituents with different chemical properties and was not possible to observe an antioxidant effect compared with standard.

On the other hand, Table 3 showed that compounds **6b**, **6c**, **6d**, and **6g** have good activity in scavenging ABTS radical, presenting better  $\text{IC}_{50}$  values than those found for ascorbic acid, used as reference. This is consistent with the results reported previously where described compounds having an electron withdrawing group like fluorine, and electron donating groups, like methoxy on the phenyl rings, exhibit good antioxidant activity (Mubeen et al., 2015; Polo et al., 2016).

Computational methods are important tools to predict some compound properties with interesting experimental biological activities, e.g, QikProp is a quick, accurate, and easy to use absorption, distribution, metabolism, and excretion (ADME) prediction program (Schrödinger, 2017). The main parameters are shown in Table 4. Taking into account the Lipinski's rule of five (molecular weight below 500 Da, hydrogen bond donor less than 5, acceptor less than 10, and Log P (octanol/water partition coefficient) for the ligand less than five), the synthesized compounds did not present violations to this rule, being within of permissible range of each descriptor (Lipinski et al., 1997). Likewise, the synthesized THQ series satisfies other parameters involved in the absorption, distribution and membrane penetration as water solubility (Log S) and polar surface area (PSA). Finally, the predicted qualitative oral absorption was calculated. This prediction is made through the analysis of the appropriate values of different descriptors. The analysis showed that the compounds could present good oral absorption. In general, the new *N*-propargyl tetrahydroquinolines presented permissible values in the different descriptors calculated (Singh et al., 2012).

To understand the biological activity reported, an analysis of chemical reactivity were developed and Quantum Similarity field and

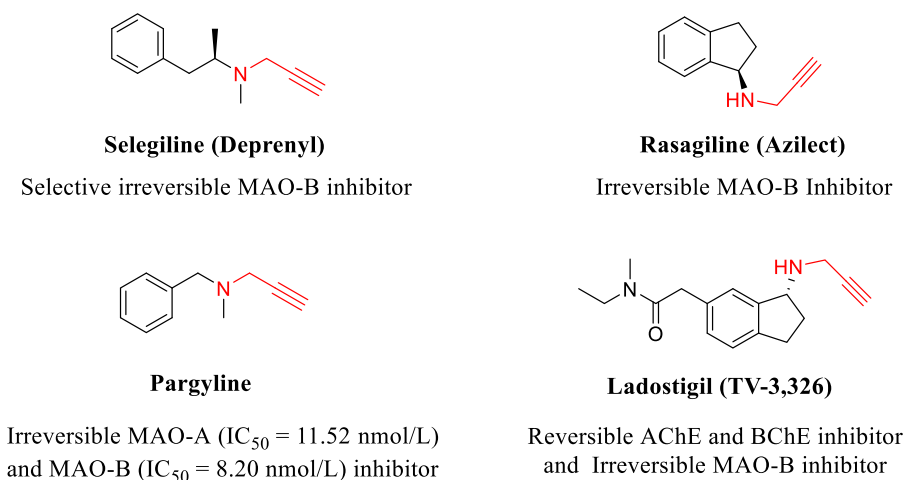
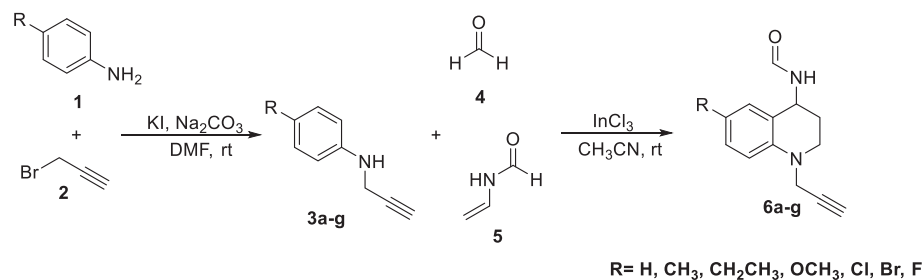


Fig. 1. Propargylamines inhibitors of monoamine oxidases MAO-A and MAO-B.



**Scheme 1.** Synthesis of *N*-propargyl THQs **6a-g** from *N*-propargylamines via domino Mannich/Friedel-Crafts alkylation reactions.

**Table 1**  
Physicochemical parameters obtained for the new THQ compounds.

| Compound  | R                               | MW (g/mol) | Time (h) | Yield (%) | m.p. (°C) <sup>a</sup> |
|-----------|---------------------------------|------------|----------|-----------|------------------------|
| <b>3a</b> | H                               | 131.17     | 3        | 51%       | Oil                    |
| <b>3b</b> | CH <sub>3</sub>                 | 145.20     | 3        | 49%       | Oil                    |
| <b>3c</b> | OCH <sub>3</sub>                | 161.20     | 3        | 48%       | Oil                    |
| <b>3d</b> | CH <sub>2</sub> CH <sub>3</sub> | 159.23     | 3        | 45%       | Oil                    |
| <b>3e</b> | Br                              | 210.07     | 3        | 51%       | Oil                    |
| <b>3f</b> | Cl                              | 165.62     | 3        | 44%       | Oil                    |
| <b>3g</b> | F                               | 149.16     | 3        | 58%       | Oil                    |
| <b>6a</b> | H                               | 214.26     | 4        | 51%       | 118–120                |
| <b>6b</b> | CH <sub>3</sub>                 | 228.29     | 4        | 95%       | 134–136                |
| <b>6c</b> | OCH <sub>3</sub>                | 244.29     | 4        | 66%       | 110–112                |
| <b>6d</b> | CH <sub>2</sub> CH <sub>3</sub> | 242.32     | 4        | 31%       | 116–118                |
| <b>6e</b> | Br                              | 293.16     | 4        | 52%       | 164–166                |
| <b>6f</b> | Cl                              | 248.71     | 4        | 23%       | 158–160                |
| <b>6g</b> | F                               | 232.25     | 4        | 71%       | 144–146                |

<sup>a</sup> Uncorrected.

**Table 2**  
% Decoloration of DPPH solution for synthesized compounds in comparison with ascorbic acid. Values are the average of triplicate experiments.

| Compound             | Concentration (µg/mL) |             |             | IC <sub>50</sub> |
|----------------------|-----------------------|-------------|-------------|------------------|
|                      | 100                   | 50          | 10          |                  |
| <b>6a</b>            | 12.63 ± 1.2           | 5.26 ± 1.5  | 1.04 ± 0.2  | >100             |
| <b>6b</b>            | 19.74 ± 3.2           | 10.52 ± 1.5 | 0.00 ± 0.0  | >100             |
| <b>6c</b>            | 45.53 ± 5.6           | 29.47 ± 4.1 | 21.05 ± 5.1 | >100             |
| <b>6d</b>            | 22.37 ± 2.4           | 16.58 ± 3.3 | 7.11 ± 2.0  | >100             |
| <b>6e</b>            | 22.63 ± 3.7           | 18.42 ± 2.5 | 6.58 ± 2.1  | >100             |
| <b>6f</b>            | 18.16 ± 5.5           | 7.89 ± 1.3  | 5.26 ± 1.2  | >100             |
| <b>6g</b>            | 20.00 ± 7.0           | 9.73 ± 0.8  | 2.8 ± 1.3   | >100             |
| <b>Ascorbic acid</b> | -                     | -           | -           | 1 ± 0.3          |

**Table 3**  
ABTS radical scavenging activity (%) of the synthesized compounds, measured at 745 nm, compared to standard ascorbic acid. Values are the average of triplicate experiments.

| Compound             | Concentration (µg/mL) |             |             | IC <sub>50</sub> |
|----------------------|-----------------------|-------------|-------------|------------------|
|                      | 100                   | 50          | 10          |                  |
| <b>6a</b>            | 90.41 ± 8.7           | 75.27 ± 6.4 | 46.27 ± 2.1 | 12.30 ± 4.2      |
| <b>6b</b>            | 98.08 ± 5.8           | 88.49 ± 6.6 | 79.32 ± 9.3 | 3.72 ± 0.7       |
| <b>6c</b>            | 93.54 ± 7.5           | 91.68 ± 5.9 | 82.30 ± 5.4 | 2.12 ± 0.8       |
| <b>6d</b>            | 94.03 ± 9.2           | 53.73 ± 5.0 | 78.46 ± 9.5 | 3.35 ± 0.5       |
| <b>6e</b>            | 81.45 ± 6.2           | 68.88 ± 4.8 | 36.93 ± 8.6 | 41.15 ± 6.3      |
| <b>6f</b>            | 86.31 ± 5.6           | 70.95 ± 6.6 | 6.85 ± 2.0  | 32.09 ± 2.5      |
| <b>6g</b>            | 92.53 ± 8.7           | 82.99 ± 8.5 | 72.82 ± 6.5 | 2.98 ± 0.7       |
| <b>Ascorbic acid</b> | -                     | -           | -           | 35 ± 2.7         |

Chemical reactivity framework were used. Taking into account the structural features of these molecular sets, which have only a substitute, the molecular quantum similarity indices allowed us to quantify the structural and electronic effects from a local point of view. The highest overlap similarity was observed between **6e** and **6b** and for **6d** and **6f**

with a value of 0.9998 in both cases (Table 5), with a Euclidean distance of 1.3725 and 0.7756 respectively (Table 6).

The most active compound **6c** has a high overlap similarity value with the compounds **6b** (0.9985), **6e** and **6f** (0.9985), with euclidean distances of 4.5485, 4.8028 and 4.2535 respectively. Compound **6c** also has a high electronic similarity with the compounds **6d** (0.9709), **6e** (0.9417), **6f** (0.9512), **6g** (0.9589) (See Table S1, supporting information) with euclidean distances of 0.9481, 1.3324, 1.2288, 1.1379, respectively (See Table S2, supporting information). These compounds **6e**, **6f**, and **6g** have strong electron withdrawing groups such as -Br, -Cl and -F compared with compound **6c** which has a methoxy group. In general, the electronic similarity values are higher than the Overlap similarity values. For this reason, chemical reactivity descriptors are reported in Table 7.

The higher chemical potential is shown for the compound **6f** ( $\mu = -3.6551$  eV), hardness ( $\eta = 7.3985$  eV), softness ( $S = 0.2735$  eV<sup>-1</sup>) and electrophilicity ( $\omega = 0.9028$  eV). The most reactive compound **6c** has chemical potential ( $\mu = -3.2856$ ), hardness ( $\eta = 7.2253$  eV), softness ( $S = 0.3043$  eV<sup>-1</sup>) and electrophilicity ( $\omega = 0.7470$  eV). These reactivity parameters of new compounds can be related to the properties as free radical scavengers.

Fig. 2 shows the Fukui Function ( $f_k^- \approx |HOMO|^2$  and  $f_k^+ \approx |LUMO|^2$ ) figures for the selected compound **6c** (most active compound, **3a** and **6a** (reference compound to series **3** and **6** respectively).

Compounds **3a** and **6a** have the same reactivity maps in both figures. These reactivity maps can be related to the retrodonor process on the non-covalent interaction for these compounds (Wenqin et al., 2015; Jørgensen, 2000). Unlike the reference compounds, the most active compound **6c** has different maps for the Fukui Functions ( $f_k^- \approx |HOMO|^2$  and  $f_k^+ \approx |LUMO|^2$ ) respectively. Therefore, the compound **6c** has zones good defined for electrophilic and nucleophilic attacks that can influence their activity. Finally, the local electrophilicity and nucleophilicity dissimilarity using DFT Based Reactivity Descriptors, to relate the chemical reactivity with the quantum similarity, are shown in Table 8. The compound **6c** has the higher local reactivity similarity (electrophilicity dissimilarity: 0.041), and the compound **6d** has the higher nucleophilicity dissimilarity:  $5.52 \times 10^{-3}$  with respect to the reference compound **6a**. These dissimilarities can be related to the zone of reactivity (the Fukui function maps, see Fig. 2) in this series of compounds.

### 3. Experimental

#### 3.1. Chemistry

All reagents were purchased from either Merck (Darmstadt, Germany) or Sigma and Aldrich Chemical Co (St. Louis, MO, USA) and used without further purification. All products were characterized by spectral data (IR, MS, <sup>1</sup>H-NMR, <sup>13</sup>C-NMR). NMR spectra (<sup>1</sup>H and <sup>13</sup>C) were measured on a Bruker Ultrashield-400 spectrometer (Rheinstetten, Germany), using CDCl<sub>3</sub> as solvent and reference. *J* values are reported in Hz;

**Table 4**  
Computer aided ADME screening of the synthesized compounds *N*-propargyl tetrahydroquinolines.

| Compound | M.W. (g/mol) | Log P (o/w) <sup>a</sup> | donors HB <sup>b</sup> | acceptors HB <sup>c</sup> | Log S <sup>d</sup> | PSA <sup>e</sup> | Human Oral Absorption <sup>f</sup> |
|----------|--------------|--------------------------|------------------------|---------------------------|--------------------|------------------|------------------------------------|
| 6a       | 214.266      | 1.628                    | 1.500                  | 3.500                     | -1.827             | 51.657           | 3                                  |
| 6b       | 228.293      | 1.882                    | 1.500                  | 3.500                     | -2.030             | 51.857           | 3                                  |
| 6c       | 244.293      | 1.697                    | 1.500                  | 4.250                     | -1.750             | 60.103           | 3                                  |
| 6d       | 242.320      | 2.230                    | 1.500                  | 3.500                     | -2.398             | 51.878           | 3                                  |
| 6e       | 293.162      | 2.068                    | 1.500                  | 3.500                     | -2.225             | 50.692           | 3                                  |
| 6f       | 248.711      | 2.068                    | 1.500                  | 3.500                     | -2.205             | 51.858           | 3                                  |
| 6g       | 232.257      | 1.725                    | 1.500                  | 3.500                     | -1.710             | 50.726           | 3                                  |

<sup>a</sup> log P for octanol/water (-2.0 - -6.5).

<sup>b</sup> Estimated number of H-bonds that would be donated by the solute to water molecules in an aqueous solution.

<sup>c</sup> Estimated number of H-bonds that would be accepted by solute from water molecules in an aqueous solution.

<sup>d</sup> Predicted aqueous solubility, log S, S in mol dm<sup>-3</sup> (-6.5 - 0.5).

<sup>e</sup> Van der Waals surface areas of polar nitrogen and oxygen atoms.

<sup>f</sup> Qualitative human oral absorption predicted: 1, 2 or 3 for low, medium or high.

**Table 5**  
Molecular quantum Similarity values using the overlap operator.

|    | 6a     | 6b     | 6c     | 6d     | 6e     | 6f     | 6g     |
|----|--------|--------|--------|--------|--------|--------|--------|
| 6a | 1.0000 |        |        |        |        |        |        |
| 6b | 0.9954 | 1.0000 |        |        |        |        |        |
| 6c | 0.9897 | 0.9985 | 1.0000 |        |        |        |        |
| 6d | 0.9895 | 0.9958 | 0.9935 | 1.0000 |        |        |        |
| 6e | 0.9957 | 0.9998 | 0.9958 | 0.9964 | 1.0000 |        |        |
| 6f | 0.9913 | 0.9995 | 0.9958 | 0.9998 | 0.9993 | 1.0000 |        |
| 6g | 0.9915 | 0.9978 | 0.9932 | 0.9952 | 0.9959 | 0.9964 | 1.0000 |

**Table 6**  
Molecular Quantum Similarity values using the Euclidean distance for the overlap operator.

|    | 6a     | 6b     | 6c     | 6d     | 6e     | 6f     | 6g     |
|----|--------|--------|--------|--------|--------|--------|--------|
| 6a | 0.0000 |        |        |        |        |        |        |
| 6b | 4.1721 | 0.0000 |        |        |        |        |        |
| 6c | 7.9565 | 4.5485 | 0.0000 |        |        |        |        |
| 6d | 7.4087 | 4.1515 | 2.2423 | 0.0000 |        |        |        |
| 6e | 3.9958 | 1.3725 | 4.8028 | 4.2161 | 0.0000 |        |        |
| 6f | 4.2546 | 1.5458 | 4.2535 | 0.7756 | 3.5410 | 0.0000 |        |
| 6g | 5.3227 | 2.8750 | 4.6077 | 5.1883 | 3.5665 | 3.0600 | 0.0000 |

**Table 7**  
Global reactivity descriptors for the compounds.

| Compound | C. Potential (μ, eV) | C. Hardness (η, eV) | Softness (S, eV) <sup>-1</sup> | Electrophilicity (ω, eV) |
|----------|----------------------|---------------------|--------------------------------|--------------------------|
| 6a       | -3.5233              | 7.8842              | 0.1268                         | 0.7873                   |
| 6b       | -3.3652              | 7.5548              | 0.2838                         | 0.7494                   |
| 6c       | -3.2856              | 7.2253              | 0.3043                         | 0.7470                   |
| 6d       | -3.3456              | 7.6528              | 0.2989                         | 0.7313                   |
| 6e       | -3.6483              | 7.3599              | 0.2741                         | 0.9042                   |
| 6f       | -3.6551              | 7.3985              | 0.2735                         | 0.9028                   |
| 6g       | -3.6085              | 7.3956              | 0.2771                         | 0.8803                   |

chemical shifts are reported in ppm (δ) relative to the solvent peak (residual CHCl<sub>3</sub> in CDCl<sub>3</sub> at 7.26 ppm for protons and 77 ppm for carbon atoms). Signals were designated as follows: s, singlet; d, doublet; dd, doublet of doublets; t, triplet; td, triplet of doublets; q, quartet; m, multiplet, and br., broad. IR spectra (KBr pellets, 500–4000 cm<sup>-1</sup>) were recorded on a NEXUS 670 FT-IR spectrophotometer (Thermo Nicolet, Madison, WI, USA). GC-MS analyses were performed on a model Trace 1300 GC-MS instrument (Thermo Fisher Scientific, Waltham, MA, USA) equipped with a Rtx-5MS on-column auto-injector and a fused silica capillary column (DB-5, 30 m × 0.25 mm ID, 0.25 μm film thickness). MS were recorded in electron ionization (EI) mode, with the energy of 70 eV. The ion source temperature was 200 °C; 4.00 min solvent cut time.

Melting points (uncorrected) were measured on an Electrothermal IA9100 melting point apparatus (Stone, Staffs, UK). The reaction progress was monitored using thin layer chromatography on PF254 TLC aluminum sheets from Merck. Column chromatography was performed using Silica gel (60–120 mesh) and Solvents employed were of analytical grade.

### 3.2. General procedure for the synthesis of *N*-propargyl-1,2,3,4-THQs

THQ derivatives were efficiently synthesized according to methodology reported previously (Rodríguez et al., 2016), the protocol outlined in Fig. 1. This protocol can be divided into two steps:

#### 3.2.1. Step 1: preparation of *N*-propargylamine

In a round-bottomed flask, a 5-mL solution in anhydrous DMF of the corresponding anilines **1** (1.8 mmol), potassium iodide (0.1 mmol) and anhydrous sodium carbonate (2 mmol) was prepared and stirred constantly at 0 °C. A solution of propargyl bromide **2** (1.0 mmol) in anhydrous DMF was added dropwise and the mixture was kept at 0 °C for 20 minutes. The reaction was allowed to stir at room temperature for 3–4 h, indicated on TLC. The reaction mixture was diluted with water and extracted with ethyl acetate (3 × 20 mL), the organic phase was separated and dried (Na<sub>2</sub>SO<sub>4</sub>), the solvent removed under vacuum and the resulting product was purified by column chromatography on silica gel, (petroleum ether: ethyl acetate) to obtain the pure *N*-propargyl anilines **3a-g**.

#### 3.2.2. Step 2: preparation of *N*-propargyl THQs

All the reactions were performed at room temperature. In a round bottom flask, a 5 mL solution in CH<sub>3</sub>CN of preformed *N*-propargylaniline **3a-g** (1.0 mmol) and formaldehyde (37% in methanol) **4** (1.1 mmol) was prepared and stirred for 10 minutes. 5 mL solution of InCl<sub>3</sub> (20% mol) in CH<sub>3</sub>CN was then added. After 20 minutes a solution of *N*-vinylformamide **5** (1.1 mmol) in CH<sub>3</sub>CN was incorporated to the reaction mixture and was vigorously stirred. The resulting mixture was stirred for 3–4 h. After the workup, the final product was purified by column chromatography, eluted with the appropriate mixture of petroleum ether and ethyl acetate to afford pure THQs **6a-g**.

#### 3.2.3. *N*-(1-prop-2-ynyl-1,2,3,4-tetrahydro-quinolin-4-yl)formamide (**6a**)

Coffee solid; m.p. 118–120 °C; Yield 51%; IR: 3279, 3038, 2958, 2922, 2847, 1658, 1492, 751; <sup>1</sup>H NMR (400 MHz, CDCl<sub>3</sub>) δ (ppm): 8.20 (1H, s), 7.22–7.31 (2H, m), 6.82–6.88 (2H, m), 5.21–5.28 (1H, m), 4.19–4.26 (1H, dd, *J* = 18.2, 1.7 Hz), 4.00–4.07 (1H, dd, *J* = 18.2, 1.1 Hz), 3.32–3.39 (2H, m), 2.25–2.28 (1H, s), 2.15–2.24 (2H, m). <sup>13</sup>C NMR (100 MHz, CDCl<sub>3</sub>) δ (ppm): 160.09, 144.57, 129.60, 129.17, 122.23, 118.11, 112.81, 79.01, 72.09, 45.24, 44.76, 40.72, 28.48; GC-MS *m/z* (rel. int. %): 213.80 (24), 174.88 (10), 167.78 (100), 129.88 (20). Anal.

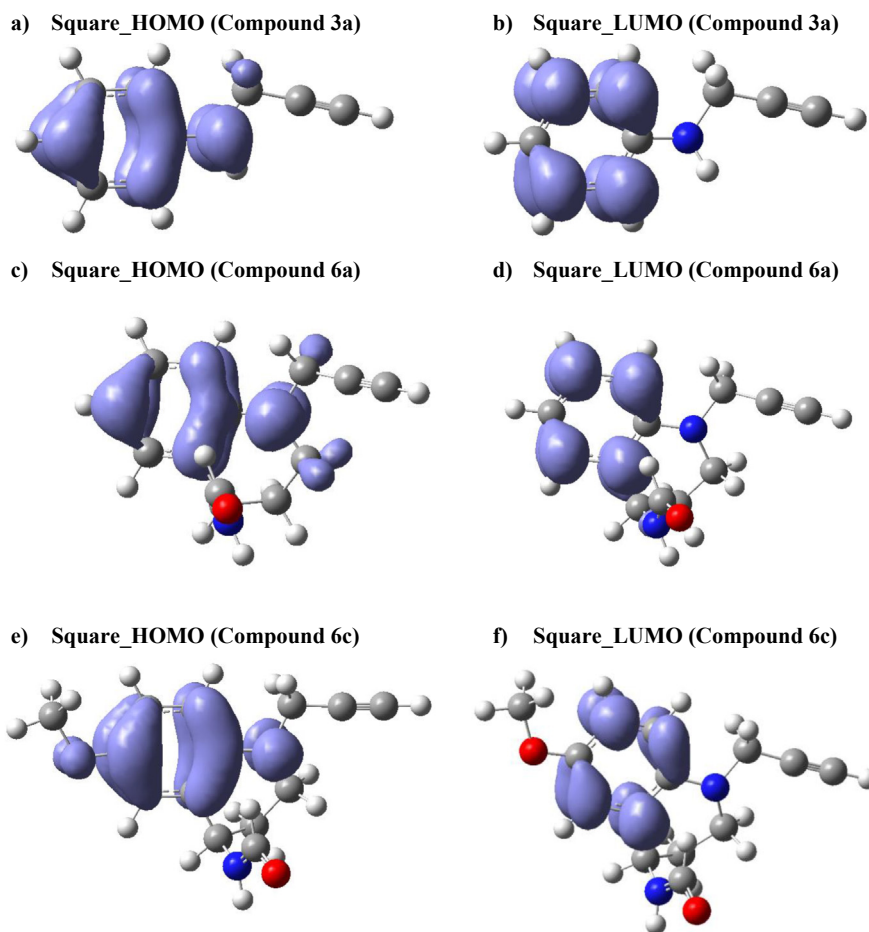


**Fig. 2.** Fukui Functions ( $f_k^- \approx |HOMO|^2$  and  $f_k^+ \approx |LUMO|^2$ ), for the compound selected **6c** (most active compound), **6a** and **3a** (reference compounds to series **6** and precursors **3** respectively).

**Table 8**  
Local electrophilicity and nucleophilicity dissimilarity.

| Reference Compound (6a) vs | Electrophilicity dissimilarity | Nucleophilicity dissimilarity |
|----------------------------|--------------------------------|-------------------------------|
| <b>6b</b>                  | $7.51 \times 10^{-3}$          | $4.09 \times 10^{-3}$         |
| <b>6c</b>                  | 0.041                          | $4.91 \times 10^{-3}$         |
| <b>6d</b>                  | $9.89 \times 10^{-3}$          | $5.52 \times 10^{-3}$         |
| <b>6e</b>                  | $3.35 \times 10^{-3}$          | $1.19 \times 10^{-3}$         |
| <b>6f</b>                  | $5.22 \times 10^{-3}$          | $4.28 \times 10^{-4}$         |
| <b>6g</b>                  | $4.29 \times 10^{-3}$          | $2.79 \times 10^{-3}$         |

Calc. for  $C_{13}H_{14}N_2O$ : 214.11 uma.

### 3.2.4. *N*-(6-methyl-1-prop-2-ynyl-1,2,3,4-tetrahydro-quinolin-4-yl)formamide (**6b**)

Orange solid; m.p. 134–136 °C; Yield 95%; IR: 3278, 2951, 2923, 2854, 1655, 1506, 1380, 1328, 1230, 803;  $^1H$  NMR (400 MHz,  $CDCl_3$ )  $\delta$  (ppm): 8.18 (1H, s), 6.97–7.05 (2H, m), 6.70 (1H, d,  $J = 8.3$  Hz), 5.16 (1H, d,  $J = 6.1$  Hz), 4.09–4.16 (1H, d,  $J = 18.1$  Hz), 3.88–3.95 (1H, d,  $J = 18.1$  Hz), 3.21–3.26 (2H, m), 2.22–2.24 (3H, s), 2.15 (1H, br), 1.99–2.14 (2H, m).  $^{13}C$  NMR (100 MHz,  $CDCl_3$ )  $\delta$  (ppm): 160.04, 142.37, 130.11, 129.74, 127.53, 122.40, 113.11, 79.08, 72.08, 45.34, 44.66, 40.86, 28.75, 20.23; GC-MS m/z (rel. int. %): 227.71 (38), 188.92 (10), 181.88 (100), 166.87 (12), 143.97 (24). Anal. Calc. for  $C_{14}H_{16}N_2O$ : 228.13 uma.

### 3.2.5. *N*-(6-methoxy-1-prop-2-ynyl-1,2,3,4-tetrahydro-quinolin-4-yl)formamide (**6c**)

Coffee solid; m.p. 110–112 °C; Yield 66%; IR: 3262, 3231, 2953,

2917, 2845, 1653, 1501, 1460, 1374, 1048, 737;  $^1H$  NMR (400 MHz,  $CDCl_3$ )  $\delta$  (ppm): 8.18 (1H, s), 6.80 (1H, dd,  $J = 8.9, 3.0$  Hz), 6.71–6.76 (2H, m), 5.17 (1H, dd,  $J = 12.9, 5.1$  Hz), 4.10 (1H, dd,  $J = 18.1, 2.2$  Hz), 3.90 (1H, dd,  $J = 18.1, 2.3$  Hz), 3.73 (3H, s), 3.18–3.22 (2H, m), 2.13–2.15 (1H, br), 2.04–2.23 (2H, m).  $^{13}C$  NMR (100 MHz,  $CDCl_3$ )  $\delta$  (ppm): 160.05, 152.33, 138.91, 123.74, 115.25, 114.57, 114.51, 79.11, 72.20, 55.71, 45.55, 44.85, 41.22, 28.94; GC-MS m/z (rel. int. %): 243.76 (80), 204.89 (12), 197.97 (100), 159.64 (28), 144.80 (16). Anal. Calc. for  $C_{14}H_{16}N_2O_2$ : 244.12 uma.

### 3.2.6. *N*-(6-ethyl-prop-2-ynyl-1,2,3,4-tetrahydro-quinolin-4-yl)formamide (**6d**)

Beige solid; m.p. 116–118 °C; Yield 31%; IR: 3273, 3231, 2951, 2923, 2849, 1648, 1506, 1376, 1331, 804;  $^1H$  NMR (400 MHz,  $CDCl_3$ )  $\delta$  (ppm): 8.11 (1H, s), 7.03 (1H, d,  $J = 8.1$  Hz), 6.97 (1H, d,  $J = 14.5$  Hz), 6.71 (1H, d,  $J = 8.4$  Hz), 5.10–5.17 (1H, m), 4.11 (1H, d,  $J = 18.1$  Hz), 3.91 (1H, d,  $J = 18.1$  Hz), 3.18–3.26 (2H, m), 2.52 (2H, q,  $J = 7.5$  Hz), 2.15 (1H, t,  $J = 6.6$  Hz), 2.03–2.13 (2H, m), 1.18 (3H, t,  $J = 7.6$  Hz).  $^{13}C$  NMR (100 MHz,  $CDCl_3$ )  $\delta$  (ppm): 160.15, 142.56, 133.99, 128.94, 128.50, 122.32, 113.02, 79.19, 72.11, 45.32, 44.70, 40.83, 28.74, 27.74, 15.74; GC-MS m/z (rel. int. %): 242.03 (34), 195.93 (100), 181.81 (12), 157.78 (22). Anal. Calc. for  $C_{15}H_{18}N_2O$ : 242.14 uma.

### 3.2.7. *N*-(6-bromo-1-prop-2-ynyl-1,2,3,4-tetrahydro-quinolin-4-yl)formamide (**6e**)

White solid; m.p. 164–166 °C; Yield 52%; IR: 3239, 3044, 2956, 2920, 2851, 1645, 1490, 1241, 891;  $^1H$  NMR (400 MHz,  $CDCl_3$ )  $\delta$  (ppm): 8.19 (1H, s), 7.21–7.25 (2H, m), 6.62 (1H, d,  $J = 9.1$  Hz), 5.15 (1H, dd,  $J$

= 11.4, 5.1 Hz), 4.07 (1H, d,  $J = 18.3$  Hz), 3.91 (1H, d,  $J = 18.2$  Hz), 3.26 (2H, t,  $J = 5.6$  Hz), 2.13–2.17 (1H, br), 1.99–2.13 (2H, m).  $^{13}\text{C}$  NMR (100 MHz,  $\text{CDCl}_3$ )  $\delta$  (ppm): 160.85, 143.81, 131.33, 131.03, 125.38, 114.35, 109.09, 78.92, 72.90, 45.90, 43.78, 40.71, 28.59; **GC-MS m/z (rel. int. %)**: 291.52 (40), 247.98 (100), 209.76 (28), 166.82 (62). *Anal. Calc. for*  $\text{C}_{13}\text{H}_{13}\text{BrN}_2\text{O}$ : 292.02 uma.

### 3.2.8. *N*-(6-chloro-1-prop-2-ynyl-1,2,3,4-tetrahydro-quinolin-4-yl) formamide (**6f**)

Beige solid; m.p. 158–160 °C; Yield 23%; **IR**: 3231, 2949, 2914, 2842, 1643, 1494, 1387, 1331, 1238;  $^1\text{H}$  NMR (400 MHz,  $\text{CDCl}_3$ )  $\delta$  (ppm): 8.21 (1H, s); 7.11–7.16 (2H, m), 6.69 (1H, d,  $J = 9.0$  Hz), 5.14–5.20 (1H, m), 4.10 (1H, d,  $J = 18.2$  Hz), 3.94 (1H, d,  $J = 18.3$  Hz), 3.20–3.25 (2H, m), 2.15–2.18 (1H, br), 2.02–2.15 (2H, m).  $^{13}\text{C}$  NMR (100 MHz,  $\text{CDCl}_3$ )  $\delta$  (ppm): 160.09, 143.15, 129.19, 128.95, 123.86, 122.84, 114.16, 78.50, 72.37, 45.43, 44.48, 40.86, 28.43; **GC-MS m/z (rel. int. %)**: 247.78 (44), 208.85 (15), 201.64 (100), 166.90 (40). *Anal. Calc. for*  $\text{C}_{13}\text{H}_{13}\text{ClN}_2\text{O}$ : 248.07 uma.

### 3.2.9. *N*-(6-fluoro-1-prop-2-ynyl-1,2,3,4-tetrahydro-quinolin-4-yl) formamide (**6g**)

Beige solid; m.p. 144–146 °C; Yield 71%; **IR**: 3273, 3257, 2954, 2915, 1650, 1503, 801;  $^1\text{H}$  NMR (400 MHz,  $\text{CDCl}_3$ )  $\delta$  (ppm): 8.19 (1H, s), 6.88–6.93 (2H, m), 6.67–6.73 (1H, m), 5.17 (1H, dd,  $J = 13.2, 5.4$  Hz), 4.08 (1H, dd,  $J = 18.2, 2.2$  Hz), 3.93 (1H, dd,  $J = 18.2, 2.2$  Hz), 3.21–3.26 (2H, m), 2.15–2.17 (1H, br), 1.99–2.20 (2H, m).  $^{13}\text{C}$  NMR (100 MHz,  $\text{CDCl}_3$ )  $\delta$  (ppm): 160.14, 141.04, 123.94, 115.78, 115.56, 114.13, 114.06, 78.74, 72.34, 45.67, 44.60, 41.16, 28.72; **GC-MS m/z (rel. int. %)**: 231.80 (28), 192.85 (10), 185.78 (100), 147.74 (30). *Anal. Calc. for*  $\text{C}_{13}\text{H}_{13}\text{FN}_2\text{O}$ : 232.10 uma.

## 3.3. Measurement of DPPH radical scavenging activity

DPPH is a stable free radical that can accept an electron or hydrogen radical to become a stable molecule. The antioxidant activity can be observed by a change of coloration deep violet to yellow in the mixture of compounds with a methanolic solution of DPPH. The hydrogen atom or electron donation ability of the compounds was measured from the bleaching of the purple colored methanol solution of DPPH (Kedare and Singh, 2011).

The free radical scavenging effect of the compounds was assessed by the discoloration of a methanolic solution of DPPH as previously reported (Polo et al., 2016). Tetrahydroquinolines **6a–g** was assayed at 100, 50 and 10  $\mu\text{g}/\text{mL}$ . The scavenging of free radicals by THQs was evaluated spectrophotometrically at 517 nm against the absorbance of the DPPH radical. The percentage of discoloration was calculated as follows:

$$\% \text{ scavenging DPPH free radical} = 100 \times (1 - \text{AE}/\text{AD})$$

Where AE, is the absorbance of the solution after adding the extract and AD is the absorbance of the blank DPPH solution. Ascorbic acid was used as reference compounds, with  $\text{IC}_{50}$  value of 1  $\mu\text{g}/\text{mL}$ .

## 3.4. Measurement of ABTS radical scavenging activity

The ABTS (2,2'-Azino-bis(3-ethylbenzothiazoline-6-sulfonic acid) radical scavenging assay is a rapid and efficient method, based on the ability of the hydrogen donating antioxidants to scavenge the long-life radical cation  $\text{ABTS}^{\bullet+}$ . In this method, the preformed radical monocation of ABTS is generated by the oxidation of ABTS with potassium persulfate and is reduced in the presence of such hydrogen donating antioxidants (Karadag et al., 2009).

ABTS assay was performed according to the protocol (Polo et al., 2016; Re et al., 1999). The ABTS radical cation ( $\text{ABTS}^{\bullet+}$ ) was produced by reaction of 7 mM stock solution of ABTS with 2.45 mM potassium persulfate and allowing the mixture to stand in dark at room temperature

for 12 h before use. The  $\text{ABTS}^{\bullet+}$  solution was diluted with methanol to give an absorbance of  $0.7 \pm 0.01$  at 745 nm. Compounds (1 mL) were allowed to react with 2 ml of the  $\text{ABTS}^{\bullet+}$  solution and the absorbance was measured at 745 nm after 1 min. Data for each assay was recorded in triplicate. Ascorbic acid was used as positive controls with  $\text{IC}_{50}$  value of 35  $\mu\text{g}/\text{mL}$ . The scavenging activity was estimated based on the percentage of ABTS radicals scavenged by the following formula:

$$\% \text{ scavenging} = [(A_0 - A_s)/A_0] \times 100$$

Where  $A_0$  is the absorption of control,  $A_s$  is the absorption of a tested compound solution.

## 3.5. In silico prediction of pharmacokinetic properties

Pharmacokinetic properties of THQ compounds were calculated an *in silico* way through ADME descriptors using QikProp (Caporuscio et al., 2011). Based on the Lipinski's rule of 5, some of the descriptors predicted were molecular weight, Van der Waals, surface areas of polar nitrogen and oxygen atoms, H bond acceptors, H bond donors, Log P (octanol/water) and aqueous solubility (Lipinski et al., 1997), proposing a first analysis of the newly synthesized compounds as drug-likeness.

## 3.6. Computational methods

The theoretical study was realized based on Molecular Quantum Similarity Measure (MQSM), density functions, analyzing a series of reactive descriptors as chemical hardness ( $\eta$ ), chemical potential ( $\mu$ ), electrophilicity index ( $\omega$ ), softness ( $s$ ), and Fukui functions. All the structures included in this study were optimized at B3LYP/6-31G(d) level of theory by using the Gaussian 09 package (Frisch et al., 2016). Detail and basis of the methods used are included in the supplementary material.

## 4. Conclusion

In summary, the synthesis of a new series of substituted *N*-propargylTHQs derivatives has been developed in mild conditions and simple procedure through the Domino Mannich/Friedel - Crafts reactions using  $\text{InCl}_3$  as catalyst. The antioxidant activity is dependent on the concentration of the compounds, likewise, the compound **6c** and **6g** (with methoxy and fluorine group on the aromatic ring respectively) presented the most favorable antioxidant activity values. Physicochemical descriptors, calculated theoretically, indicated that the new compounds have a low toxicity risk. Structurally the *N*-propargyl THQs are attractive for the production of a second generation of compounds due to the reactivity of the propargyl fragment. In this study, we obtained compounds with higher antioxidant capacity than the reference compound. From the theoretical calculations (MQSM, Global reactivity descriptors, and Fukui Functions), we can establish similarity and discriminate different reactive sites in the new molecules where the oxidative process occurs. These sites can be used for the design of new compounds with interesting biological activity.

## Declarations

### Author contribution statement

Y Rodríguez: Conceived and designed the experiments; Performed the experiments; Analyzed and interpreted the data; Wrote the paper.

A Romero: Conceived and designed the experiments; Wrote the paper.

M Gutiérrez: Conceived and designed the experiments; Performed the experiments; Analyzed and interpreted the data; Contributed reagents, materials, analysis tools or data; Wrote the paper.

M Norambuena: Performed the experiments.

A Morales: Performed the experiments; Analyzed and interpreted the data; Contributed reagents, materials, analysis tools or data; Wrote the paper.

#### Funding statement

This work was supported by the Institute of Chemistry of Natural Resources, University of Talca, Chile and PIEI QUIMBIO project, UTalca.

#### Competing interest statement

The authors declare no conflict of interest.

#### Additional information

Supplementary content related to this article has been published online at <https://doi.org/10.1016/j.heliyon.2019.e02174>.

#### References

- Aruoma, O.I., 1998. Free radicals, oxidative stress, and antioxidants in human health and disease. *J. Am. Oil Chem. Soc.* 75 (2), 199–212.
- Abonia, R., Castillo, J., Insuasty, B., Quiroga, J., Nogueiras, M., Cobo, J., 2013. Efficient catalyst-free four-component synthesis of novel  $\gamma$ -aminoethers mediated by a Mannich type reaction. *ACS Comb. Sci.* 15 (1), 2–9.
- Acelas, M., Bohórquez, A.R.R., Kouznetsov, V.V., 2017. Highly diastereoselective synthesis of new trans-fused octahydro-acridines via intramolecular cationic imino diels–alder reaction of *N*-protected anilines and citronellal or citronella essential oil. *Synthesis* 49 (10), 2153–2162.
- Baranyi, M., Porceddu, P.F., Goloncsér, F., Kulcsár, S., Otrócski, L., Kittel, A., Pinna, A., Frau, L., Huleatt, P.B., Khoo, M.L., Chai, C.L., Dunkel, P., Matyus, P., Morelli, M., Sperlagh, B., 2016. Novel (Hetero)arylalkenyl propargylamine compounds are protective in toxin-induced models of Parkinson's disease. *Mol. Neurodegener.* 11 (6), 015–0067.
- Bolea, I., Gella, A., Unzeta, M., 2013. Propargylamine-derived multitarget-directed ligands: fighting Alzheimer's disease with monoamine oxidase inhibitors. *J. Neural Transm.* 120 (6), 893–902.
- Bulut, N., Kocyigit, U.M., Gecibesler, I.H., Dastan, T., Karcı, H., Taslimi, P., Sevgi, D., İlhami, G., Cetin, A., 2018. Synthesis of some novel pyridine compounds containing bis-1, 2, 4-triazole/thiosemicarbazide moiety and investigation of their antioxidant properties, carbonic anhydrase, and acetylcholinesterase enzymes inhibition profiles. *J. Biochem. Mol. Toxicol.* 32 (1).
- Caporuscio, F., Rastelli, G., Imbriano, C., Del Río, A., 2011. Structure-based design of potent aromatase inhibitors by high-throughput docking. *J. Med. Chem.* 54 (12), 4006–4017.
- Dragoni, S., Porcari, V., Travagli, M., Castagnolo, D., Valoti, M., 2006. Antioxidant properties of propargylamine derivatives: assessment of their ability to scavenge peroxynitrite. *J. Pharm. Pharmacol.* 58 (4), 561–565.
- Frisch, M.J., Trucks, G.W., Schlegel, H.B., Scuseria, G.E., Robb, M.A., Cheeseman, J.R., Scalmani, G., Barone, V., Petersson, G.A., Nakatsuji, H., Li, X., Caricato, M., Marenich, A., Bloino, J., Janesko, B.G., Gomperts, R., Mennucci, B., Hratchian, H.P., Ortiz, J.V., Izmaylov, A.F., Sonnenberg, J.L., Williams-Young, D., Ding, F., Lipparini, F., Egidi, F., Goings, J., Peng, B., Petrone, A., Henderson, T., Ranasinghe, D., Zakrzewski, V.G., Gao, J., Rega, N., Zheng, G., Liang, W., Hada, M., Ehara, M., Toyota, K., Fukuda, R., Hasegawa, J., Ishida, M., Nakajima, T., Honda, Y., Kitao, O., Nakai, H., Vreven, T., Throssell, K., Montgomery Jr., J.A., Peralta, J.E., Ogliaro, F., Bearpark, M., Heyd, J.J., Brothers, E., Kudin, K.N., Staroverov, V.N., Keith, T., Kobayashi, R., Normand, J., Raghavachari, K., Rendell, A., Burant, J.C., Iyengar, S.S., Tomasi, J., Cossi, M., Millam, J.M., Klene, M., Adamo, C., Cammi, R., Ochterski, J.W., Martin, R.L., Morokuma, K., Farkas, O., Foresman, J.B., Fox, D.J., 2016. Gaussian 09, Revision A.02. M., Wallingford, CT.
- Hua, R., Nizami, T.A., 2018. Synthesis of heterocycles by using propargyl compounds as versatile synthons. *Mini-Reviews Org. Chem.* 15 (3), 198–207.
- Jørgensen, K.A., 2000. Catalytic asymmetric hetero-diels–alder reactions of carbonyl compounds and imines. *Angew. Chem. Int. Ed.* 39 (20), 3558–3588.
- Karadag, A., Ozcelik, B., Saner, S., 2009. Review of methods to determine antioxidant capacities. *Food. Anal. Method* 2 (1), 41–60.
- Katritzky, A.R., Rachwal, S., Rachwal, B., 1996. Recent progress in the synthesis of 1,2,3,4-tetrahydroquinolines. *Tetrahedron* 52 (48), 15031–15070.
- Kedare, S.B., Singh, R.P., 2011. Genesis and development of DPPH method of antioxidant assay. *J. Food. Sci. Tech. Mys.* 48 (4), 412–422.
- Kouznetsov, V.V., Gómez, C.M.M., Parada, L.K.L., Bermudez, J.H., Méndez, L.Y.V., Acevedo, A.M., 2011. Efficient synthesis and free-radical scavenging capacity of new 2,4-substituted tetrahydroquinolines prepared via BiCl<sub>3</sub>-catalyzed three-component Povarov reaction, using *N*-vinylamides. *Mol. Divers.* 15 (4), 1007.
- Lauder, K., Toscani, A., Scalacci, N., Castagnolo, D., 2017. Synthesis and reactivity of propargylamines in organic chemistry. *Chem. Rev.* 117 (24), 14091–14200.
- Lipinski, C.A., Lombardo, F., Dominy, B.W., Feeney, P.J., 1997. Experimental and computational approaches to estimate solubility and permeability in drug discovery and development settings. *Adv. Drug Deliv. Rev.* 23 (1–3), 3–25.
- Mao, F., Li, J., Wei, H., Huang, L., Li, X., 2015. Tacrine-propargylamine derivatives with improved acetylcholinesterase inhibitory activity and lower hepatotoxicity as a potential lead compound for the treatment of Alzheimer's disease. *J. Enzym. Inhib. Med. Chem.* 30 (6), 995–1001.
- Martelli, G., Giacomini, D., 2018. Antibacterial and antioxidant activities for natural and synthetic dual-active compounds. *Eur. J. Med. Chem.* 158, 91–105.
- Mubeen, M., Kini, S.G., Pai, K.S.R., 2015. Design, synthesis, antioxidant and anticancer activity of novel pyrazole derivatives. *Der. Pharm. Chem.* 7 (2), 215–223.
- Nammalwar, B., Bunce, A.R., 2014. Recent syntheses of 1,2,3,4-tetrahydroquinolines, 2,3-dihydro-4(1H)-quinolinones and 4(1H)-Quinolinones using domino reactions. *Molecules* 19 (1).
- Polo, E., Trilleras, J., Ramos, J., Galdámez, A., Quiroga, J., Gutierrez, M., 2016. Efficient MW-assisted synthesis, spectroscopic characterization, X-ray and antioxidant properties of indazole derivatives. *Molecules* 21 (7).
- Re, R., Pellegrini, N., Proteggente, A., Pannala, A., Yang, M., Rice-Evans, C., 1999. Antioxidant activity applying an improved ABTS radical cation decolorization assay. *Free Radic. Biol. Med.* 26 (9–10), 1231–1237.
- Rodríguez, Y.A., Gutierrez, M., Ramirez, D., Alzate-Morales, J., Bernal, C.C., Guiza, F.M., Romero Bohórquez, A.R., 2016. Novel *N*-allyl/propargyl tetrahydroquinolines: synthesis via three-component cationic imino diels-alder reaction, binding prediction, and evaluation as cholinesterase inhibitors. *Chem. Biol. Drug Des.* 88 (4), 498–510.
- Romero Bohórquez, A., Romero-Daza, J., Acelas, M., 2016. Versatile and mild HCl-catalyzed cationic imino Diels-Alder reaction for the synthesis of new tetrahydroquinoline derivatives. *Synth. Commun.* 46 (4).
- Singh, K.D., Kirubakaran, P., Nagarajan, S., Sakthiah, S., Muthusamy, K., Velmurgan, D., Jeyakanthan, J., 2012. Homology modeling, molecular dynamics, e-pharmacophore mapping and docking study of Chikungunya virus nsP2 protease. *J. Mol. Model.* 18 (1), 39–51.
- Sridharan, V., Suryavanshi, P.A., Menéndez, J.C., 2011. Advances in the chemistry of tetrahydroquinolines. *Chem. Rev.* 111 (11), 7157–7259.
- Schrödinger, 2017. Release 2017-3. LigPrep, S., LLC, New York, NY.
- Wenqin, X., Wei, W., Xiang, W., 2015. Gold-catalyzed cyclization leads to a bridged tetracyclic indolenine that represses beta-lactam resistance. *Angew. Chem., Int. Ed. Engl.* 54 (33), 9546–9549.
- Yang, Y., Hu, Z.L., Li, R.H., Chen, Y.H., Zhan, Z.P., 2018. Pyrazole synthesis via a cascade Sonogashira coupling/cyclization of *N*-propargyl sulfonylhydrazones. *Org. Biomol. Chem.* 16 (2), 197–201.